FULL 360° AZIMUTH ANGLE WIDEBAND PROPAGATION MODELING FOR AN URBAN LINE-OF-SIGHT MICROCELLULAR ENVIRONMENT

Hassan M. El-Sallabi [1], Wei Zhang [2], Kimmo Kalliola [3], and Pertti Vainikainen [4]
Radio Laboratory, Institute of Radio Communications
Helsinki University of Technology
P. O. Box 3000, FIN-02015 HUT, Finland
E-mail: [1]hel@radio.hut.fi, [2]WZH@radio.hut.fi, [3]kka@radio.hut.fi, [4]pva@radio.hut.fi

Abstract — **This paper presents the 360° azimuth angle channel modeling of wideband propagation in urban line-of-sight (LOS) microcellular environment of array antennas at the basestation and its experimental validations. First, the modeling includes rays from whole 360° azimuth angles. Second, it verifies that the use of three-dimensional and two-dimensional methods in forward and other reflection and diffraction propagation directions, respectively, is appropriate for the LOS propagation predictions. Third, it includes reflections from curved surfaces of street corners and walls. Fourth, it extends existing expressions, making them applicable for array antennas at the basestation. The results compared with wideband measurements provide better understanding of the propagation mechanism.**

I. INTRODUCTION

This paper presents a deterministic site-specific modeling based on specular reflection and uniform geometrical theory of diffraction (UTD) which are important tools for the predictions of mobile radio propagation [1-9]. The purpose of this work is 1) to model wide-band propagation in urban line-of-sight (LOS) microcellular environments for array antennas at the basestation, 2) to verify the use of three-dimensional (3-D) and two-dimensional (2-D) methods for propagation predictions in forward (transmitter to receiver) and other reflection and diffraction propagation directions, respectively, is appropriate, and 3) to study frequency correlation properties of wideband channel which is important for the beamforming of adaptive array antennas.

II. MEASUREMENT SETUP

The measurements were carried out in the city center of Helsinki, Finland. The measurement system consists of a wideband channels sounder of a single receiver and a radio frequency (RF) switch that separates received signals from eight receiving antennas. Fig. 1 shows block diagram of the system [12]. The spacing between antennas is a half wavelength. The prototype antenna hardware was made in such a way that measurement can be carried out appropriately in every 60-degree sector. To obtain full 360° azimuth coverage, the measurement was performed in six 60° sectors. The measured impulse responses from eight antennas are used to estimate parameters of wideband propagation. The transmitter and receiver antennas are nearly at the same height. The carrier frequency of the sounder is f_o = 2.154 GHz. The chip frequency is f_c = 53.85 MHz giving delay resolution of about 20 ns [12]. Polarization is vertical.

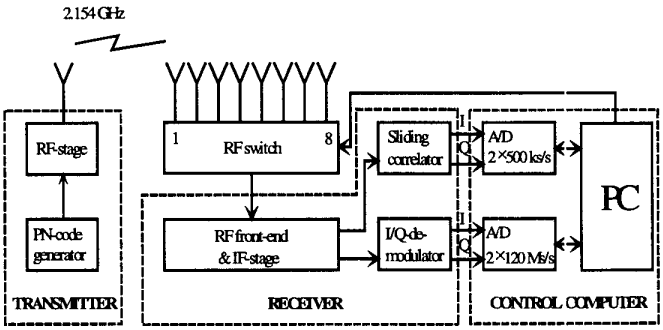

Fig. 1. Block diagram of the measurement system.

III. DIRECTIONAL CHANNEL TRANSFER FUNCTION

Let $\mathbf{H}(f,\varphi)$ be the narrow-band vector channel (multiple-antenna) transfer function for uplink, where f is the frequency and φ is the azimuth angle of arrival [10],[11]. The function $\mathbf{H}(f,\varphi)$ has been derived. A contribution of this work is the inclusion of reflections from curved surfaces which have higher amplitudes than diffraction. The reflection angle at the curved surface may be estimated by a half of the angle between the incoming from mobile station (MS) and the foregoing to the basestation (BS) directions of the ray. The reflection can be calculated by using the well-known Fresnel reflection coefficient [1-3], [7-9]. The measurements [12] and modeling cover the whole 360° azimuth angles in six 60° sectors. Specifically, 0° is the direction parallel to the main street, opposite to the transmitter, and the counting direction is clockwise. The basestation has eight antennas [12], arranged as a uniform linear array, and it receives signals from a mobile user.

0-7803-5284-X/99/$10.00 © 1999 IEEE.

The magnitude of the wideband channel transfer function defines narrow-band path loss L_n as in [2],[3],[5] and it also gives indication of the frequency selective fading channel. Fig. 2 presents L_n results for the six sectors at frequency range $f_o \pm f_c$, where f_o=2.154 GHz and f_c=53.85 MHz are the carrier and shift register clock frequencies [5],[12], respectively. The number of extremes is determined by $2f_c/\Delta f_{ik}$ at $\Delta f_{ik} = 1/|\tau_i - \tau_k|$, $(i \neq k = 1,2,3,\ldots,M)$, where τ_i and τ_k are time delays of rays i and k. For sector 180° the direct ray path length $r_d \approx 100$m and the triple reflection ray path length $r_{3r} \approx 115$m yield $\Delta f_{ik} \approx 20$ MHz, the number of extremes is about 5. Indeed, 5 extremes appear in Fig. 2.

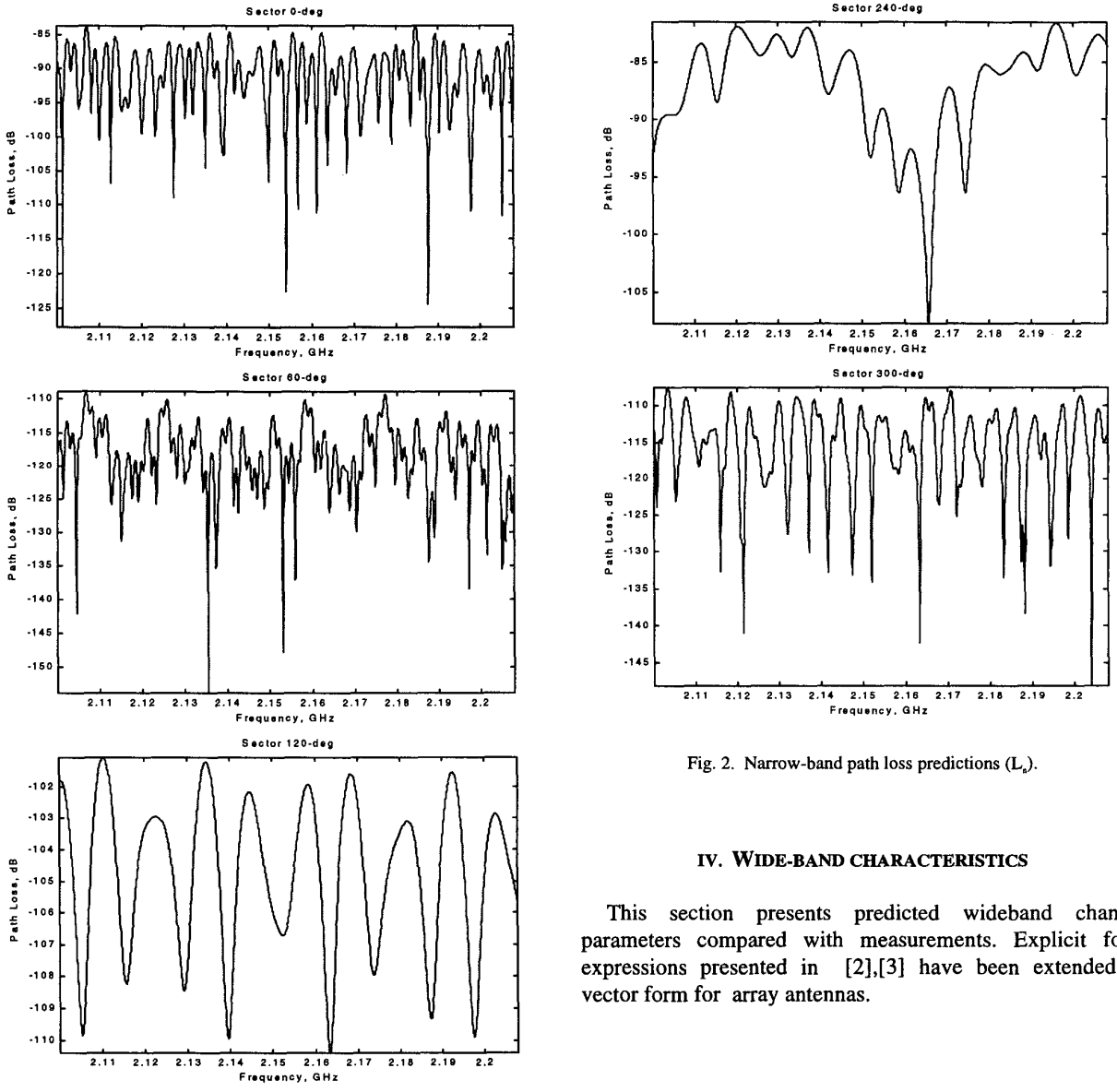

Fig. 2. Narrow-band path loss predictions (L_n).

IV. WIDE-BAND CHARACTERISTICS

This section presents predicted wideband channel parameters compared with measurements. Explicit form expressions presented in [2],[3] have been extended to vector form for array antennas.

a) Spatial-Temporal Domain Path Loss

Both measurements and predictions of spatial-temporal domain path loss are presented in Fig. 3. The directions of arrival (DOA) are estimated from measurement results using Fourier processing [12]. The Chebychev amplitude taper weighting for -25 dB side lobe level is applied. Although Fourier processing is not a high resolution technique, it is a practical aspect and simple in computation. The angular resolution is 15°. The DOA used in modeling are obtained from measurement site geometry. In order to compare with measurements, the same Fourier processing technique has been applied for model prediction. Rays from the crossing street junction corners between transmitter and receiver contribute to the arrive signals in the angle ranges 90°-150° and 210°-270°.

The time domain path loss $L_p(t)$ physically interprets and reasonably predicts the power delay profiles. Fig. 4 presents the $L_p(t)$ calculations for the first element of the array antennas and the corresponding measurement results. Predictions for all eight elements have been obtained. There is no significant difference between different elements. The number of rays needed in the forward direction is less than that in other reflection and diffraction propagation directions. The difference between their peak values is about 10 dB.

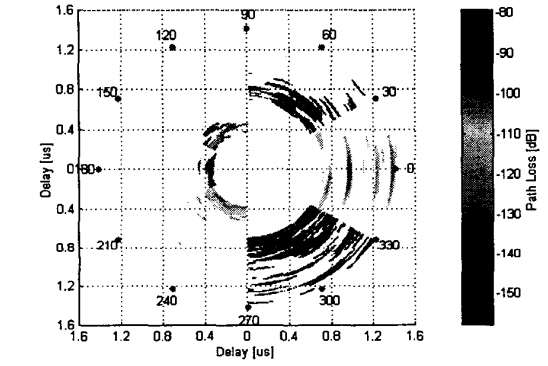

(a)

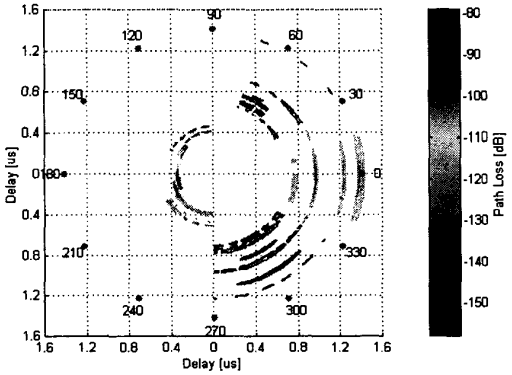

(b)

Fig. 3. (a) Measured and (b) predicted path loss in temporal-spatial domain.

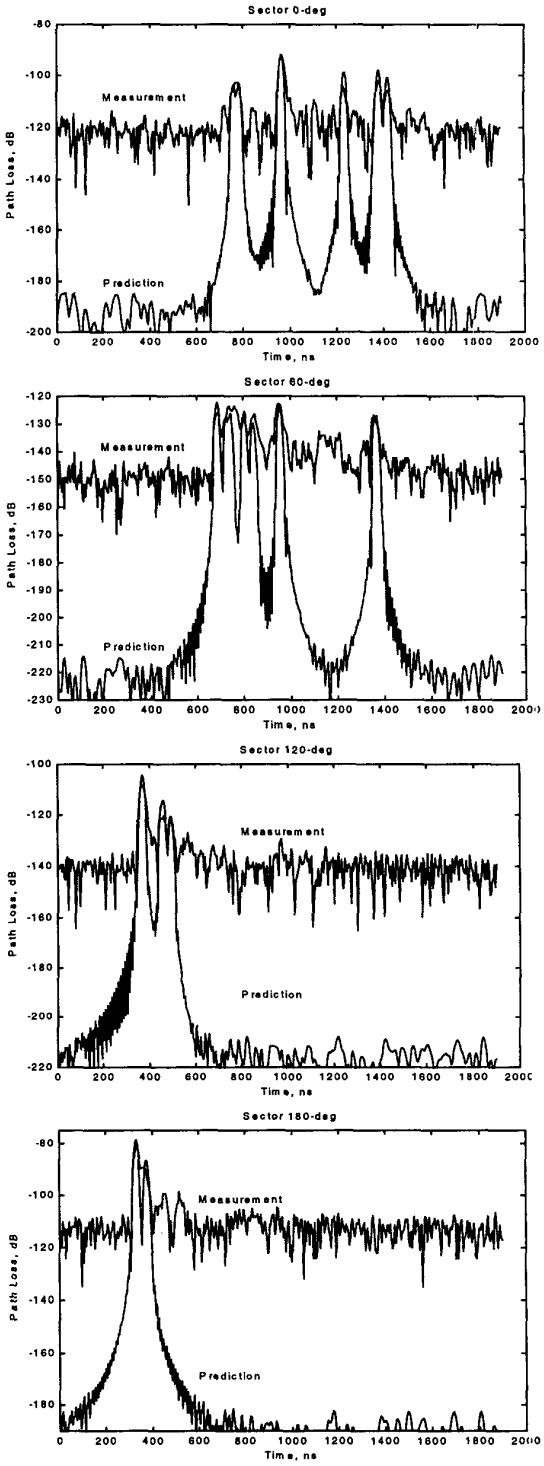

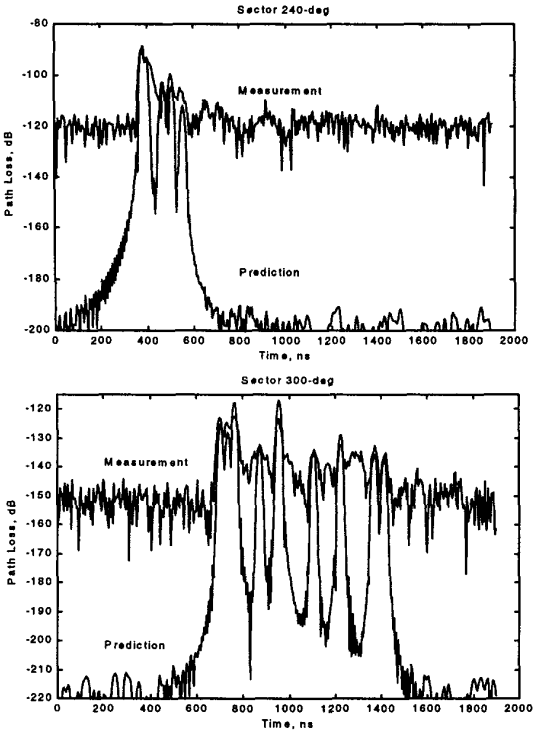

Fig. 4. Measured and calculated time-domain path loss.

b) Relative Power in Frequency Domain

Fig. 5 presents relative power P(f) of measurements and model prediction for sectors 0° and 180° corresponding to the results presented in Fig. 4. Results for all elements and sectors have been obtained. The agreements between measurements and predictions are good. Indeed P(f) spans a frequency band FB= $4f_c$ = 215.4 MHz. It is anticipated and reasonable that the main spectral lobe of P(f) appears in a finite bandwidth W = $2f_c$.

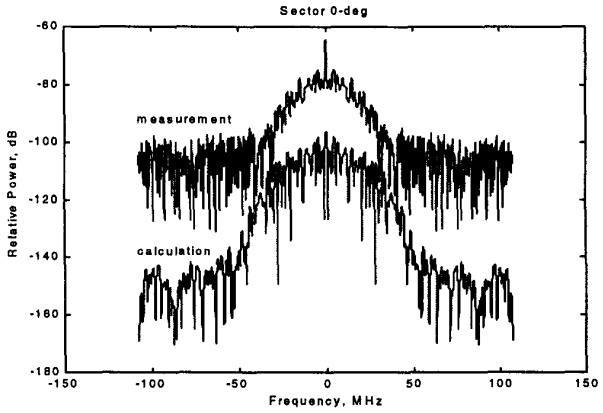

(a)

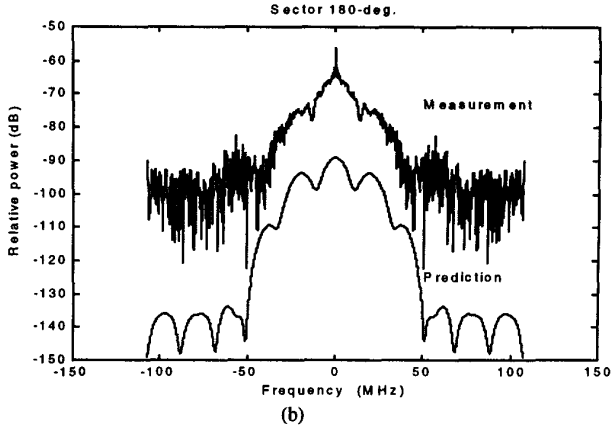

(b)

Fig. 5. Relative power in frequency domain for (a)-sector 0° and (b) sector 180° corresponding to the results presented in Fig. 3. The measured curve displaced above by 25 dB to facilitate comparison.

c) Frequency Correlation

Fig. 6 presents the magnitude of predicted frequency correlation function and that derived from measurements of sector 0°. The magnitude is equivalent to the correlation between the complex envelopes of two continuous wave (CW) signals separated in frequency. Low correlation is evidenced as the frequency separation increases. This is due to frequency dependent of the channel.

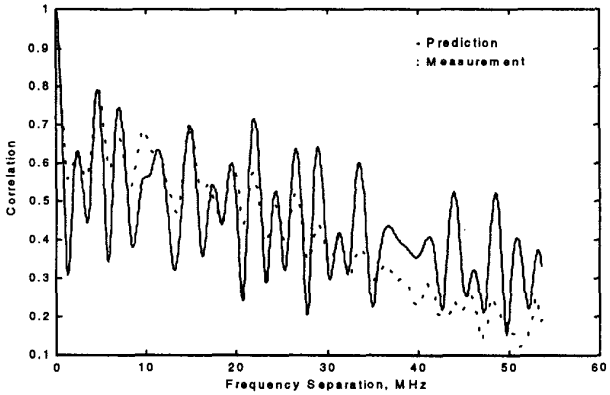

Fig. 6. Magnitude of channel frequency correlation function of sector 0°.

d) Wide-Band Path Loss

Explicit form expressions presented in [2],[3] have been used in the calculations of wideband path loss. Table I summarizes the predicted and measured results, where M_W and C_W are the measured and calculated Wideband path loss, L_m and L_p are the measured and predicted peak values of time-domain path loss, and L_n is the narrow-band path loss at the specified frequency.

TABLE I: Numerical values of measured and calculated path loss of the first element of the antennas for all six sectors.

Sector	Model (rays)	M_W (dB)	C_W (dB)	L_c (dB)	L_s (dB)	$L_s(f_c-f_s)$ (dB)	$L_s(f_c)$ (dB)	$L_s(f_c+f_s)$ (dB)
0°	6	-94.9	-89.5	-92.3	-92.0	-88.5	-115.5	-96.1
60°	7	-127.0	-116.7	-122.7	-122.1	-117.9	-119.3	-123.9
120°	3	-110.6	-104.2	-108.3	-104.7	-101.8	-105.9	-104.7
180°	4	-85.5	-78.1	-81.2	-78.8	-77.8	-79.2	-77.07
240°	5	-89.5	-87.1	-93.6	-88.7	-93.2	-89.6	-83.6
300°	9	-125.4	-113.4	-122.5	-116.8	-112.2	-111.6	-114.4

V. Conclusion

This work presents the 360° azimuth angle range wideband propagation modeling of an urban LOS microcellular environment for array antennas at the basestation. The results compared with wideband measurements provide better understanding of the propagation mechanism. First, 2-D method is used for the inclusion of more reflection and diffraction rays. Corner diffraction is significant in the propagation directions with arrival angles within 90°-150° and 210°-270°. Second, the modeling includes reflections from curved surfaces. Third, the vector channel transfer function has been derived. Fourth, the extension of existing explicit-form expressions has made these expressions applicable for array antennas at the basestation.

Acknowledgment

This work was supported by the Academy of Finland and by Technology Development Center (TEKES), Finland. The authors would like to thank Prof. A. Räisänen for his encouragement. The first author was financially supported in part by Nokia Foundation.

References

[1] H. L. Bertoni, W. Honcharenko, L. R. Maciel and H. H. Xia, "UHF propagation for wireless personal communications," *Proc. IEEE*, vol. 82, pp. 1333 - 1359, Sep. 1994.

[2] W. Zhang, "A wide-band propagation model based on UTD for cellular mobile radio communications," *IEEE Trans. Antennas and Propagat.*, vol. 45, pp. 1669-1678, Nov. 1997.

[3] W. Zhang, "Physical modeling of wide-band propagation for urban line-of-site micro-cellular mobile and personal communications," *Journal of Electromagnetic Waves and applications*, vol. 11, pp. 1633-1648, Dec. 1997.

[4] A. G. Kanatas, I. D. Kounouris, G. B. Kostaras and P. Constantinou, "A UTD propagation model in urban microcellular environments," *IEEE Trans. Veh. Technol.*, vol. 46, pp. 185-193, Jan. 1997.

[5] R. J. Luebbers, W. A. Foose and G. Reyner, " Comparison of GTD propagation model wideband path loss simulation with measurements," *IEEE Trans. Antennas and Propagat.*, vol. 37 pp. 499-505, Apr. 1989.

[6] R. G. Kouyoumjian and P. H. Pathk, "A uniform geometrical theory of diffraction for and edge in a perfectly conducting surface," *Proc. IEEE*, vol. 62, pp. 1448-1461, Nov. 1974.

[7] S. Y. Tan and H. S. Tan, "A microcellular communications propagation model based on the uniform theory of diffraction and multiple image theory," *IEEE Trans. Antennas and Propagat.*, vol. 44, pp.1317-1326, Oct. 1996.

[8] K. Rizk , J.-F. Wagen and F. Gardiol "Two-dimensional ray-tracing modeling for propagation in microcellular environments, ' *IEEE Trans. Veh. Technol.*, vol. 46, pp. 508-518, Feb. 1997.

[9] H. H. Xia, H. L. Bertoni, L. R. Macial, A. L.-Stewart and Row, "Radio propagation characteristics for line-of-sight microcellular and personal communications," *IEEE Trans. Antennas and Propagat.*, vol. 41 pp. 1439-1447, Oct. 1993.

[10] J. Fuhl, J.-P. Rossi and E. Bonek "High-resolution 3-D direction of arrival determination for Urban mobile radio," *IEEE Trans. Antennas and Propagat.*, vol. 45, pp. 672- 682, Apr. 1997.

[11] J.-P. Rossi, J.-P Barbot and A. J. Levy "Theory and measurement of the angle of arrival and time delay of UHF radiowaves using a ring array," *IEEE Trans. Antennas and Propagat.*, vol. 45, pp. 876-884, May 1997.

[12] K. Kalliola and P. Vainikainen, "Characterization system for radio channel adaptive array antennas," in *Proceedings of the 8th IEEE International Symposium on Personal, Indoor and Mobile Radio Communications*, Helsinki, Finland, Sep. 1-4, 1997, pp. 95-99 .